between 22.3°W and 23.3°W.
11. D. Sandwell, *Eos* **76**, 149 (1995).
12. We determined the moment tensor in 1-mHz bands from 1 to 11 mHz, using the free-oscillation inversion method described by M. A. Riedesel, T. H. Jordan, A. F. Sheehan, and P. G. Silver [*Geophys. Res. Lett.* **13**, 609 (1986)]; no significant frequency dependence of the source mechanism was observed, which implies that the slow component of the 1994 Romanche Transform earthquake had a radiation pattern similar to that of the main shock. The mechanism labeled LF in Fig. 5 is the average across the frequency band 3 to 6 mHz. The source mechanisms of subevents A and B, also shown in Fig. 5, were determined by waveform analysis. They are similar but not identical; for example, their long-period *P*-wave polarities are reversed at Naña, Peru (NNA).
13. Although rupture velocities of shallow-focus earthquakes have been known to exceed the local shear-wave speed [R. Archuleta, *J. Geophys. Res.* **89**, 4559 (1984)], they are rare. Typical rupture velocities of shallow-focus earthquakes are less than 3.5 km/s (*14*).
14. C. H. Scholz, *The Mechanics of Earthquake Faulting* (Cambridge Univ. Press, Cambridge, 1990).
15. E. Bonatti, *et al.*, *J. Geophys. Res.* **99**, 21779 (1994); R. C. Searle, M. V. Thomas, E. J. W. Jones, *Mar. Geophys. Res.* **16**, 427 (1994). The morphology of the western portion of the Romanche Transform is extremely complex, exhibiting multiple paleotransform valleys that resulted from past changes in plate motions. The seismic gap on the main transform trace between 22.3°W and 23.3°W (Fig. 4) corresponds to a bathymetric high, which Searle *et al.* attributed to transpression caused by the northeastward bending of the fault trace at the western end of the gap. Locking of the main trace in this region could explain the offset of the B-subevent rupture to the north.
16. We obtained the spectral estimates in Fig. 6 using the procedures described in (*2–4*). We measured the spheroidal free oscillations from vertical-component seismograms in the band from 1 to 19 mHz, using the methods of P. G. Silver and T. H. Jordan [*Geophys. J. R. Astron. Soc.* **70**, 755 (1982)] and M. A. Riedesel and T. H. Jordan [*Bull. Seismol. Soc. Am.* **79**, 85 (1989)]. Measurements of first-orbit Rayleigh waves (1 to 10 mHz) and long-period body wave trains (10 to 50 mHz) were obtained from vertical-component seismograms by the methods of Ihmlé *et al.* (*3*). In all cases, synthetic seismograms were used to account for radiation-pattern and propagation effects. The synthetics were computed by mode summation from the Harvard CMT (*7*) and the degree-12 aspherical earth structure of W.-J. Su, R. L. Woodward, and A. M. Dziewonski [*J. Geophys. Res.* **99**, 6945 (1994)]. We also corrected fundamental modes above 7 mHz for smaller scale heterogeneity using the degree-36 phase-velocity maps of G. Ekström, J. Tromp, and E. W. Larson [*Eos* **74**, 438 (1993)].
17. We inverted the data using the quadratic programming algorithm of Ihmlé *et al.* (*3*), which minimizes a linear combination of a χ^2 measure of data misfit and a quadratic form measuring the smoothness of the source time function, subject to the constraint that the source time function be nonnegative. The smoothing varied from high values before the subevent-A origin time ($110 \leq t < 0$ s), which ensured that the precursor did not generate significant high-frequency arrivals, to low values during the main-shock phase of the rupture ($16 \leq t < 45$ s), when the high-frequency amplitudes were largest; intermediate values of smoothing were assumed between the initiation of subevent A and the initiation of subevent B ($0 \leq t < 16$ s) and in the interval after the main shock ($40 \leq t < 200$ s).
18. W. L. Ellsworth and G. C. Beroza [*Science* **268**, 851 (1995)] have shown that the nucleation phases for typical earthquakes release about 0.5% of the total static moment M_0 and that the duration of nucleation varies as $M_0^{1/3}$. These scaling relations yield a nucleation phase with a moment of about 1.5×10^{17} Nm and a duration of about 2 s for an earthquake the size of the 1994 Romanche Transform main shock.
19. For a rectangular fault of depth D slipping at a constant particle velocity $\Delta\dot{u}$ and growing unilaterally at a rupture velocity v_r, the moment rate will increase at a rate $\dot{M} = 2\,\mu\,Dv_r\Delta\dot{u}$, where μ is the shear modulus. The observed moment acceleration for the slow precursor of the Romanche Transform earthquake is about 1.8×10^{17} Nm/s^2. For $D = 10$ km and $\mu = 3 \times 10^{10}$ Pa, we obtain $v_r\,\Delta\dot{u} \approx 3$ m^2/s^2. Hence, if $v_r \approx 100$ m/s, $\Delta\dot{u} \approx 0.03$ m/s. In contrast, the observations for ordinary earthquakes, including the main shock of this event (Fig. 5), yield $v_r\,\Delta\dot{u} > 1000$ m^2/s^2.
20. We thank H. Webb for assistance with the gravity data and G. Ekström, J. Tromp, and E. Larson for the use of their unpublished phase-velocity maps. We are grateful to D. Wiens and an anonymous reviewer for helpful comments that improved the manuscript. Sponsored by NSF under grant EAR-9305081 and by NASA under grant NAG5-1905. P.F.I. was supported in part by the Swiss National Science Foundation.

18 June 1996; accepted 8 August 1996

A Long Pollen Record from Lowland Amazonia: Forest and Cooling in Glacial Times

P. A. Colinvaux,* P. E. De Oliveira,† J. E. Moreno, M. C. Miller, M. B. Bush‡

A continuous pollen history of more than 40,000 years was obtained from a lake in the lowland Amazon rain forest. Pollen spectra demonstrate that tropical rain forest occupied the region continuously and that savannas or grasslands were not present during the last glacial maximum. The data suggest that the western Amazon forest was not fragmented into refugia in glacial times and that the lowlands were not a source of dust. Glacial age forests were comparable to modern forests but also included species now restricted to higher elevations by temperature, suggesting a cooling of the order of 5° to 6°C.

The Amazon lowlands in glacial times are widely thought to have been much drier than at present, even according to the "refuge hypothesis," so dry as to have prevented forest from occupying much of the basin (*1*), although this view has its critics (*2–6*). Many paleoecological data suggest cooling as a major climatic forcing in the Neotropics (*7–10*). We have tested the ice-age aridity and cooling hypotheses, using proxy data from Amazonian lake sediments (*11*).

Lake Pata lies below the 300-m contour on the Hill of the Six Lakes, a low inselberg of ancient plutonic rocks at 0°16′N, 66°41′W in the Amazon lowland of northwestern Brazil (*12*) (Fig. 1). The lowland vegetation of the region is dense tropical rain forest (DTRF) in a hot, humid climate (*13*).

All the lakes on the inselberg occupy small closed, steep-sided basins with flat or shelving bottoms under 7 to 15 m of water. The water level of one lake fell by about a meter in the 2 weeks of our visit, suggesting that the basins might not be completely sealed. The water is soft and acidic, which shows that these are not carbonate solution basins. A plausible hypothesis is that these are pseudo-karst lakes occupying basins formed by the solution of silica from ancient quarzitic rocks, perhaps dating from pre-Pleistocene times (*12*).

Lake Pata is about 300 m long and 7 m deep, and it occupies a large part of its forested catchment. We piston-cored the lake at its deepest point, reaching basement gravel under 7 m of lacustrine sediment. Seven accelerator mass spectrometer (AMS) radiocarbon dates, together with five β-decay dates, demonstrate that sedimentation has been continuous, roughly constant, and extremely slow, with an age of 30,000 years being reached in the first meter (*14*) (Table 1). The gross stratigraphy is simple: a surface unit (A) of soft blackish gyttja about 60 cm thick that grades over several centimeters into a yellower, firmer, and more granular unit (B) 20 cm thick, which in turn grades into a unit (C) of bluish black

P. A. Colinvaux, J. E. Moreno, M. B. Bush, Smithsonian Tropical Research Institute, Post Office Box 2072, Balboa, Panama (mail from the United States should be sent to the Smithsonian Tropical Research Institute, Unit 0948, APO AA 34002, USA).
P. E. De Oliveira, Field Museum, Roosevelt Road at Lake Shore Drive, Chicago, IL 60605, USA.
M. C. Miller, Department of Biology, University of Cincinnati, Cincinnati, OH 45221, USA.

*To whom correspondence should be addressed.
†Present address: Institute of Geosciencies-DPE, Universidade de Sao Paulo, Rua do Lago 562, 05508-900 Sao Paulo, SP Brazil.
‡Present address: Department of Botany, Duke University, Durham, NC 27708, USA.

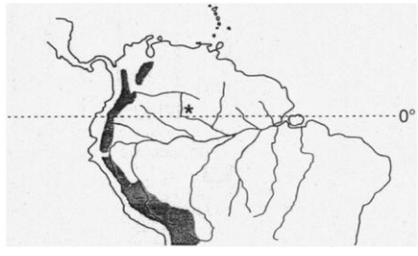

Fig. 1. Location map of the Hill of the Six Lakes (star) at 0°16′N, 66°41′W.

gyttja 5 m thick (*15*). All three stratigraphic units are represented in the last 42,000 years, spanned by the top 1.6 m of deposit (left of Fig. 2).

The obvious causal hypothesis for the stratigraphy rests on fluctuations of the lake level, with the yellowish unit B representing lowered lake level that permitted oxidation of surface mud. Four AMS dates define the boundaries of unit B as 14,230 ± 60 and 30,830 ± 220 years before present (B.P.), respectively (Table 1 and Fig. 2). These dates confirm that unit B spans the last glacial maximum (LGM) but are not exactly coincident with SPECMAP stage 2 (12,000 and 24,000 years) (*16*). Possibly the climate of the central Amazon corresponds more closely with the stage 3.1 boundary (SPECMAP 28,000 years) and the onset of late glacial warming at 14,000 years.

Figure 2 is a pollen percentage diagram for the top 1.6 m of the Lake Pata sediments, based on counts of about 500 grains per level (*17*). Between 70 and 90% of all spectra are of tree pollen, the list of identified genera (Table 2) being strongly suggestive of the DTRF certainly represented by the upper pollen spectra of the Holocene. Grass (Gramineae) pollen is present in only trace amounts, and the sum total of herbs is low to trivial, conclusive evidence that savannas or other grasslands were never present on or near the inselberg at any of the times investigated (*18*).

The pollen data, therefore, unequivocally demonstrate that closed tropical rain forest occupied the inselberg and the surrounding lowlands throughout the time spanned by the section, that is, from at least isotope stage 3 to the present (*19*). It is noteworthy that forest was maintained throughout isotope stage 2 and the LGM, despite the evidence from unit B that the lake level was lower then. Apparently the change in water balance, through a direct reduction of precipitation, lengthening of dry season, or lowering of water table, was not sufficient to disrupt the forest. The moisture regime remained within the tolerance of most rain forest taxa.

Rather than aridity, the pollen data indicate cooling in both isotope stages 2 and 3, the strongest signal being given by the tropical gymnosperm *Podocarpus* (*20*). *Podocarpus* is present in significant percentages in all sediments of isotope stages 2 and 3, reaching 10% at the LGM, but is reduced to trace amounts in the Holocene spectra. Associated with *Podocarpus* are the cool-adapted taxa *Humiria* and Ericaceae, as well as maxima of *Weinmannia*, *Ilex*, Melastomataceae, *Hedyosmum*, and *Rapanea* (expanded scales at the left of Fig. 2). Maxima of these taxa are superimposed on the pollen spectra of the rain forest: thus, the data do not require a replacement of vegetation types but rather a former enrichment of the forest with species populations now confined or prominent at higher elevations.

These pollen spectra of glacial times may be compared with glacial age pollen spectra in the western Amazon of Ecuador, where *Podocarpus*, *Weinmannia*, and even *Alnus* and *Drymis* were incorporated into Amazonian forests, although their modern altitudinal limits are Andean (>1000 m higher) (*8*). Comparable descents of temperature-sensitive taxa into lowland forests have been recorded from Panama (*10*). The *Podocarpus* and associated taxa thus invite the hypothesis that they represent entry into lowland rain forests of significant populations of more cold-adapted plants.

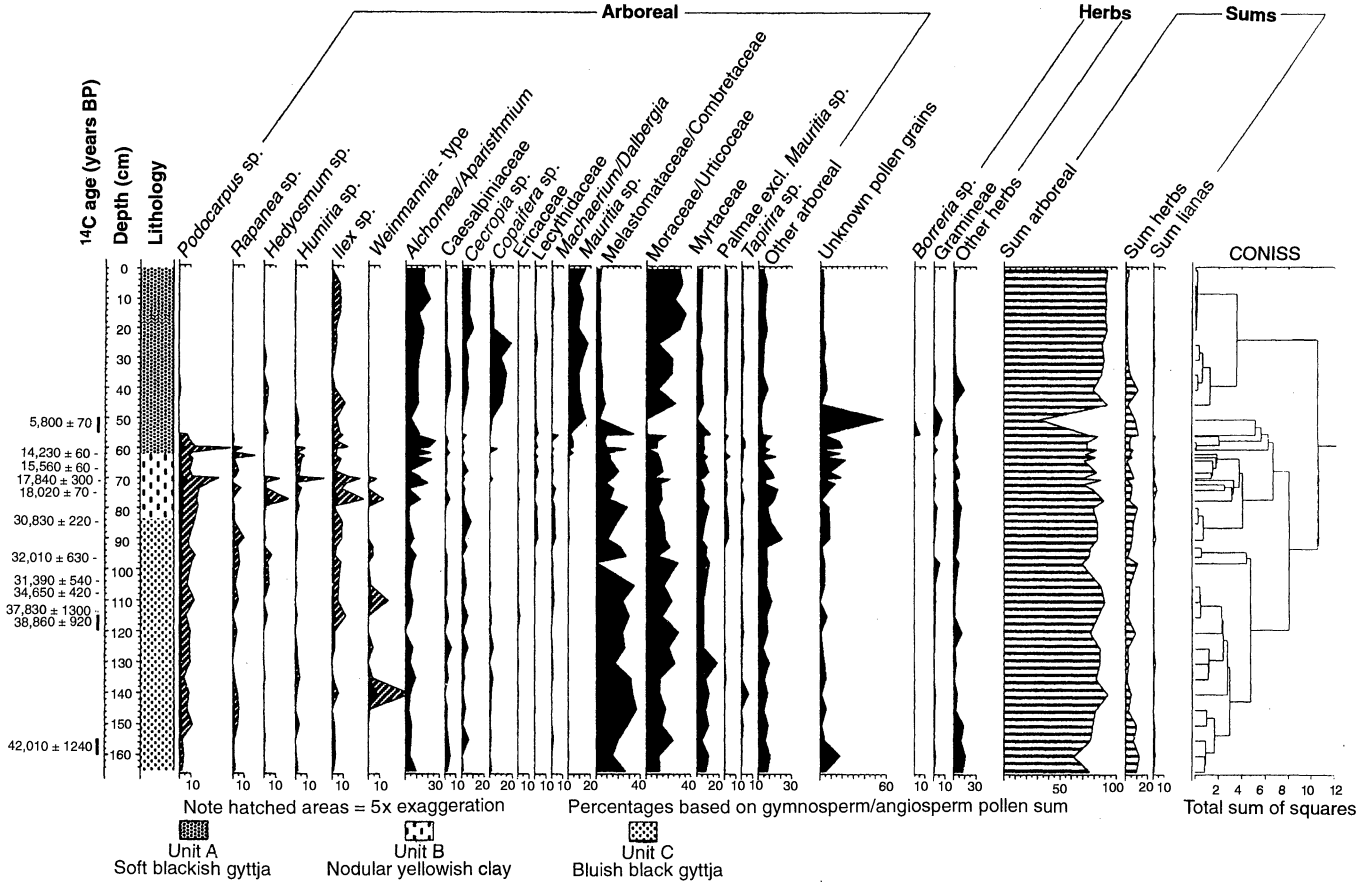

Fig. 2. Pollen percentage diagram of the top 1.6 m of sediments from Lake Pata. Data represent the percentages of total pollen. The diagonal shading of the six curves at the far left denotes that the data were amplified five times for taxa carrying the signal for glacial cooling. CONISS cluster analysis and pollen plotting by TILIA (*23*).

Applying moist air lapse rates to a *Podocarpus* descent of 800 to 1000 m from Pico da Neblina (*20*) yields temperature depression on the order of 5° to 6°C. This is of the same order as the temperature depression calculated for eastern Brazil, Amazonian Ecuador, lowland Panama, Guatemala, and the Barbados sea surface (*7–10*). At Lake Pata, temperature change probably is also responsible for the history of the palm *Mauritia*, which became prominent only with Holocene warming (*21*).

This long, continuous pollen record from the Amazon lowlands represents data from but a single site in an immense ecosystem (*11*). Nevertheless, it suggests that current views about the vegetation and climate of the ice age Amazon should be reconsidered. Although precipitation was reduced in the colder glacial times, the reduction was not sufficient to displace or fragment the rain forest. Savannas probably did not expand into what are now forested lowlands, and alternatives to the refuge hypothesis are required to explain species endemisms (*3*, *4*). Arid regions as sources of ice age dust should be sought outside the Amazon basin. We suggest that the primary environmental forcing of the Amazon system in glacial times was a drop in temperature, a direct consequence of which was an increase in diversity as rain forest communities accommodated more cool-adapted taxa as well as their present array (*7*).

Table 1. Radiocarbon dates from Lake Pata sediments. The topmost data are conventional (β-decay) dates on the first two sections of a 7-m core. Data at the bottom are AMS dates on a parallel 1-m section that overlaps the first two core sections to include sediment at the section change lost during recovery. Ages are given as uncorrected years B.P.

Sample	Age (years B.P.)	Depth (cm)
	First core (β decay)	
β-63417	5,800 ± 70	50–55
β-75109	17,840 ± 300	72–77
β-75110	31,390 ± 540	105–110
β-68529	38,860 ± 920	115–120
β-68530	42,010 ± 1240	155–160
	Parallel core (AMS)	
β-91489	14,230 ± 60	62.5
β-90306	15,560 ± 60	67.5
β-90307	18,020 ± 70	73.5
β-91490	30,830 ± 220	84.5
β-88941	32,010 ± 630	96.5
β-89715	34,650 ± 420	106.5
β-88942	37,830 ± 1300	113.5

Table 2. Arboreal genera identified in Lake Pata sediments. This list included genera with species adapted to different climatic regimes, as well as those more restricted to a tropical rain forest. *Guarea* and *Cedrela* (Meliaceae), *Clusia* (Guttiferae), and *Didymopanax* (Araliaceae) are strongly suggestive of a tropical rain forest, as are a number of grains we assigned to Bombacaceae without being able to classify them to genus. *Caryocar* is a genus mostly of forest trees (a large specimen overshadowed our camp in the forest), although one species is also prominent in cerrado vegetation, and other genera such as *Cordia, Protium, Byrsonima*, and *Pera* have many drought-tolerant species as well as moist forest species. The complete list, however, is diagnostic of a closed tropical forest.

Alchornea-Aparisthmium	*Mauritia*
Apeiba	*Mabea*
Byrsonima	*Machaerium-Dalbergia*
Caryocar	*Macrolobium*
Cassia	*Matayba*
Cecropia	*Pera*
Cedrela	*Pouteria*
Chrysophyllum	*Protium*
Clusia	*Psychotria*
Cordia	*Rapanea*
Cryosophila	*Roupala*
Didymopanax	*Sapium*
Diospyros	*Sebastiana*
Eschweilera	*Spondias*
Guarea	*Tabebuia*
Hedyosmum	*Tapirira*
Humiria	*Trattinickia*
Ilex	*Trichilia*
Iriartea	*Virola*
Luehea	*Vochysia*

REFERENCES AND NOTES

1. J. Haffer, *Science* **165**, 131 (1969); *Avian Speciation in Tropical South America* (Nuttall Ornithological Club, Cambridge, 1974); G. T. Prance, *Biological Diversification in the Tropics* (Columbia Univ. Press, New York, 1982); J. Tricart, *INQUA Supp. Bull. 265* (1974); T. C. Whitmore and G. T. Prance, *Biogeography and Quaternary History in Tropical America* (Oxford Univ. Press, Oxford, 1987); C. M. Clapperton, *Quaternary Geology and Geomorphology of South America* (Elsevier, Amsterdam, 1993); T. van der Hammen and M. L. Absy, *Palaeogeogr. Palaeoclimatol. Palaeoecol.* **109**, 247 (1994).
2. J. A. Endler, *Geographic Variation, Speciation, and Clines* (Princeton Univ. Press, Princeton, NJ, 1977); J. Salo, *Ann. Zool. Fenn.* **24**, 203 (1987); P. A. Colinvaux, *Nature* **278**, 399 (1979); S. Beven, E. F. Connor, K. Beven, *J. Biogeogr.* **11**, 383 (1984); J. D. Lynch, in *Analytical Biogeograph*, A. A. Myers and P. S. Giller, Eds. (Chapman & Hall, London, 1988), pp. 311–342; G. Irion, *Trop. Ecol.* **23**, 76 (1982).
3. M. B. Bush, *J. Biogeogr.* **21**, 5 (1994).
4. P. A. Colinvaux, in *Biological Relationships Between Africa and South America*, P. Goldblatt, Ed. (Yale Univ. Press, New Haven, CT, 1993), pp. 473–499.
5. ———, *Quat. Sci. Rev.* **6**, 98 (1987).
6. A hypothesis that the Amazon forest was replaced by glacial "Lake Amazonas" is discounted by the attribution of the postulated lacustrine features to the Miocene [M. E. Räsänen, A. M. Linna, J. C. R. Santos, F. R. Negri, *Science* **269**, 386 (1995)].
7. P. A. Colinvaux *et al.*, *Clim. Change* **32**, 19 (1996).
8. K-b. Liu and P. A. Colinvaux, *Nature* **318**, 556 (1985); M. B. Bush *et al.*, *Quat. Res.* **34**, 330 (1990).
9. M. Stute *et al.*, *Science* **269**, 379 (1995); T. P. Guilderson, R. G. Fairbanks, J. L. Rubenstone, *ibid.* **263**, 663 (1994); B. W. Leyden *et al.*, *Geophys. Monogr. Am. Geophys. Union* **78**, 165 (1993).
10. M. B. Bush and P. A. Colinvaux, *J. Veg. Sci.* **1**, 105 (1990); M. B. Bush *et al.*, *Ecol. Monogr.* **62**, 251 (1992).
11. Paleoecological and paleoclimatological research in the Amazon based on the use of proxy data from lake sediments are in their infancy, with data from <20 lowland lakes being available for even the later Holocene (*5*, *22*). Most studies have not as yet used multiproxy data, instead concentrating on exploring the possibilities of pollen analysis (*17*). A marsh core from Serra Carajas [M. L. Absy *et al.*, *C.R. Acad. Sci.* **312**, 673 (1991)] is from a savanna plateau between 700 and 900 m (*7*), and two lacustrine profiles of glacial age within the western Amazon rain forest cover only a few millennia (*8*). The sediments of Lake Pata are the first from an existing Amazonian rain forest lake found to span to glacial times. An attempt at a multiproxy examination by standardized methods at a grid of lake cores for the whole Amazon basin is being organized as a PAGES [the paleoclimate program of the International Geosphere Biosphere Program (IGBP)] contribution to the Large-Scale Biosphere-Atmosphere Experiment in Amazonia, a collaboration between NASA and the Brazilian space agency INPE. This program will include core storage for public access to cores. The Lake Pata core has been returned to Brazil in accord with government regulations.
12. C. B. Gomes, E. Ruberti, L. Morbidelli, *J. S. Am. Earth Sci.* **3**, 51 (1990); L. C. Justo and M. M. Souza, *Jazida de Nióbio do Morro dos Seis Lagos, Amazonas, Capítulo XXXVII, Principais Depósitos Minerais do Brasil, vol. 2* (Departamento Nacional da Produção Mineral, Rio de Janeiro, 1984). Deep rock drilling discovered carbonatite deposits below 225 m, but no calcareous deposits at shallower depths. Lake water is extremely soft: 2 to 5 μS; pH 4 to 4.5; no detectable dissolved sulfate: color, 50 ptn (platinum units); temperature, 28° to 30°C; oxygen and light close to zero at 3 m.
13. The regional climate is Köppen Af, equatorial, hot, and without a pronounced dry season. The average annual precipitation is 2914 mm (São Gabriel da Cachoeira) to 3652 mm (Missao Taraqua). The average annual temperature is 25°C (high, 30°C; low, 21°C) [*Radambrasil* **11**, Rio de Janeiro (1976)]. Vegetation below an elevation of 600 m is described by the vegetation map of Brazil, Dir. Geociencias, Rio de Janiero, and the *Radambrasil* maps of the Amazon as DTRF. Our own travels confirm that DTRF occupies the lowlands with an elevation of ~100 m surrounding the low inselberg. On parts of the Hill of the Six Lakes, exposed rocks and shallow soils provide edaphic constraints, suggesting that the facies of DTRF on the inselberg itself should be sensitive to changes in precipitation.
14. Comparable rates of sedimentation were measured in the two other lakes on the inselberg that we cored, Lake Dragão and Lake Verde.
15. The core was raised in meter sections from a raft of rubber boats with a piston sampler operated by push rods inside casing. Our practice is to take parallel cores from a single station, the second being depth offset by ~0.5 m, thus ensuring that any sediment lost from the bottom of a core tube during recovery is represented in the parallel core. Because of this precaution, we were able accurately to reconstruct the top 2 m of the Lake Pata sedimentary sequence even though 23 cm (including the unit B–unit C transition) were lost from the bottom of the first section of core. This lost section is present in the parallel core, where the whole of unit B, with both the unit A–unit B and the unit B–unit C transitions, is present in a single 1-m core barrel. Seven AMS dates on that single section range from 37,000 to 14,000 years; the depth-age plot being linear indicates almost constant sedimentation over this long interval (Table 1). The parallel sections (which were taken about 1 m apart) were aligned by the distinctive unit A–unit B boundary, and the alignment was checked by independent radiocarbon dating of both (for example, the AMS date of 18,020 years B.P. at 73.5 cm in the parallel section compared with a β-decay date of 17,840 years at 72 to 77 cm in the first section, Table 1).
16. J. D. Imbrie *et al.*, in *Milankovitch and Climate*, A. L. Berger *et al.*, Eds. (Reidel, Dordrecht, Netherlands, 1984), pp. 269–305.
17. Amazonian pollen analysis started late because of the forbidding taxon list (80,000 known species of vascular plants), together with the expectation that the rarity

of wind pollination mechanisms would result in minimal pollen deposition. Amazon lake mud, however, turns out to have high pollen concentrations, consistent with the high pollen influx (20,000 grains cm^{-2} $year^{-1}$) measured in our airborne-pollen traps from Ecuadorian Amazonia, from near Manaus, and from the coastal rain forest of eastern Brazil [M. B. Bush, *J. Veg. Sci.* **3**, 275 (1992)]. The Amazon pollen assemblies are extremely diverse by temperate standards (we recognized 169 taxa in the Lake Pata analyses, based on our reference collection of >5000 neotropical species in >1500 genera. This high influx of diverse pollen taxa certainly holds a remarkably detailed history of Amazonian forest associations, the full potential of which will be realized only when more autecological information is available.

18. Forest signatures are also inherent in the percentages of the more copious pollen-producing families in the forest such as Moraceae, Urticaceae, Melastomataceae, and Myrtaceae. If these percentages, together with the percentages of wind-blown pollen of grasses, are used, it is possible statistically to separate the principal plant associations of the lowland neotropics, providing an independent identification of DTRF in the Lake Pata pollen spectra [M. B. Bush, *Holocene* **1**, 162 (1991)].
19. Pollen counts at coarse intervals reveal similar forest spectra throughout the bottom 5 m of the section also, suggesting that DTRF was the local vegetation throughout the complete glacial cycle.
20. *Podocarpus* pollen has never been recorded in more than trace amounts in surface samples or Holocene sections from lowland forests of the Neotropics (*22*). The few grains of *Podocarpus* in surface and Holocene records can best be explained as the result of wind transport over long distances from *Podocarpus* stands at high elevations in the Andes and elsewhere or from rare *Podocarpus* trees in gallery forests [M. L. Salgado-Labouriau, *Proceedings of the International Conference on Aerobiology*, Berlin (1978), p. 89. Our 3 years of pollen trap data (100 traps) in Ecuadorian Amazonia include almost no *Podocarpus*. Traps in a 1-ha plot of coastal rain forest of southeastern Brazil (1 year of data, H. Behling, unpublished data) yielded only 0.8% *Podocarpus* despite the fact that three *Podocarpus* trees grow within the plot. Thus, *Podocarpus* populations much denser than those now found in Neotropical lowlands would be required to account for high *Podocarpus* pollen percentages. All reports of significant *Podocarpus* populations in northwestern Brazil are from Pico da Neblina, a mountain rising to 3014 m, 90 km northeast of the Hill of the Six Lakes. Principal herbarium holdings from the region are at the Field Museum and the New York Botanic Garden, both of which we searched for *Podocarpus*, finding minimum recorded elevations as follows: *P. bucholzii*, 2100 m; *P. magnifolius*, 1725 m; *P. roraimae*, 1200 m; *P. steyermarkii*, 1200 m; and *P. tepuiensis*, 1100 m. If the Lake Pata *Podocarpus* pollen represents descents of these populations, minimal descents were 800 m to the summit of the Hill of the Six Lakes and 1000 m to the surrounding lowlands.
21. M. B. Ribeiro, thesis, University of Brasilia (1994).
22. M. L. Absy, thesis, University of Amsterdam (1979); K-b. Liu and P. A. Colinvaux, *J. Biogeogr.* **15**, 231 (1988); M. B. Bush and P. A. Colinvaux, *Vegetatio* **76**, 141 (1988); P. A. Colinvaux *et al.*, *Rev. Palaeobot. Palynol.* **55**, 73 (1988); I. Frost, *Ecology* **69**, 66 (1988); R. A. Grabandt, *Rev. Palaeobot. Palynol.* **29**, 65 (1980).
23. E. C. Grimm, *Comput. Geosci.* **13**, 13 (1987).
24. We thank the Brazilian Council of Scientific and Technological Development for permission to work in the Amazon in collaboration with Universidade Federal do Amazonas (15 August 1990). This work was funded by National Science Foundation grant BSR-9007019, the National Geographic Society, and the Mellon Foundation.

13 May 1996; accepted 5 August 1996

Achievement of Thermal Stability by Varying Metabolic Heat Production in Flying Honeybees

Jon F. Harrison,* Jennifer H. Fewell, Stephen P. Roberts, H. Glenn Hall

Thermoregulation of the thorax allows endothermic insects to achieve power outputs during flight that are among the highest in the animal kingdom. Flying endothermic insects, including the honeybee *Apis mellifera*, are believed to thermoregulate almost exclusively by varying heat loss. Here it is shown that a rise in air temperature from 20° to 40°C causes large decreases in metabolic heat production and wing-beat frequency in honeybees during hovering, agitated, or loaded flight. Thus, variation in heat production may be the primary mechanism for achieving thermal stability in flying honeybees, and this mechanism may occur commonly in endothermic insects.

Like many other large endothermic insects, honeybees regulate thoracic temperatures relatively closely over a range of air temperatures (*1–4*). Thoracic thermoregulation in flying honeybees is thought to occur primarily through varying evaporative heat loss, which is made possible by the extrusion of nectar carried during foraging (*1–5*). Thermoregulation during flight by varying heat production has been considered implausible for endothermic insects because metabolic rates increase with rising thoracic temperature during warm-up (*1*) and because the power output required during flight has been considered to be determined by aerodynamic rather than thermoregulatory needs (*1, 2, 6*).

We discovered evidence for a thermal effect on the metabolic rate of honeybees in high-intensity, agitated flight during a study of African, European, and hybrid honeybees (*7*). In these assays, bees were agitated continuously during the measurements to elicit high-intensity flight. Both flight metabolic rate and wing-beat frequency were negatively correlated with air temperature (*8*). Flight metabolic rates were 25% lower at 30°C than at 20°C, with air temperature accounting for 47% of the measured variation in metabolic rate and 12% of the variation in wing-beat frequency over this small thermal range, despite the genetic diversity of the bees (Fig. 1). For these analyses, data from African, European, and hybrid colonies were pooled, because genotype did not significantly affect the slope of the regression relations between air temperature and metabolic rate or wing-beat frequency.

We conducted an experimental test of these correlative data by flying European honeybees at a range of air temperatures within a temperature-controlled room at the apiary of the University of California, Davis. Outgoing foragers were collected from two colonies, and flight metabolic rates, wing-beat frequencies, and thoracic and abdominal temperatures were measured (*8–10*). Honeybee thoracic temperature varied much less than ambient temperature (Fig. 2). Abdominal temperatures closely tracked air temperatures (Fig. 2), supporting previous findings that variable heat transfer between thorax and abdomen is not an important mechanism of thermoregulation in flying honeybees (*1, 3–5*). Metabolic rates of flying agitated bees decreased by 50% as air temperature rose from 20° to 40°C (Fig. 3A). Metabolic rates were unaffected by nectar loads greater than 50% of body mass at either 21° or 38°C (*11*) (Table 1), suggesting that agitated honeybees fly at near-maximal performance (*7*) and that loaded bees also thermoregulate by varying metabolic heat production.

Variation in metabolic rates with temperature for the agitated bees, which fly rapidly and erratically about the respirometry chamber, might reflect varying degrees of agitation and intensity of flight performance. Hovering flight is considered to be a well-defined behavior, in which metabolic rate is determined solely by the aerodynamic power requirements for hovering (*1, 2, 5*). We tested the effect of air temperature on the metabolic rate of bees in undisturbed hovering flight, with the expectation that the metabolic rate during hovering would be independent of air temperature (*12*). However, the metabolic rates of honeybees in stationary, undisturbed hovering flight decreased by 40% as air temperature rose from 20° to 40°C (Fig. 3A). Heinrich measured flight metabolic rates for hovering honeybees that were 20 to 40% below ours and independent of air temperature (*4*). However, by using a flow-through respirometry sys-

J. F. Harrison, J. H. Fewell, S. P. Roberts, Department of Zoology, Arizona State University, Tempe, AZ 85287-1501, USA.
H. G. Hall, Department of Entomology and Nematology, Building 970, Hull Road 0740, University of Florida, Gainesville, FL 32611–0620, USA.
*To whom correspondence should be addressed.